TOXICOLOGICAL SCIENCES **115(2)**, 557–568 (2010)
doi:10.1093/toxsci/kfq072
Advance Access publication March 8, 2010

Astrocyte-Specific Overexpression of Nrf2 Protects Striatal Neurons from Mitochondrial Complex II Inhibition

Marcus J. Calkins,* Marcelo R. Vargas,† Delinda A. Johnson,*,† and Jeffrey A. Johnson*,†,‡,§,[1]

*Molecular and Environmental Toxicology Center, †Division of Pharmaceutical Sciences, ‡Waisman Center and §Center for Neuroscience, University of Wisconsin, Madison, Wisconsin 53705

[1] To whom correspondence should be addressed at Division of Pharmaceutical Sciences, University of Wisconsin, 6125 Rennebohm Hall, 777 Highland Avenue, Madison, WI 53705. Fax: (608) 262-5345. E-mail: jajohnson@pharmacy.wisc.edu.

Received January 11, 2010; accepted February 28, 2010

Nuclear factor E2-related factor 2 (Nrf2) is a transcription factor that is known to regulate a variety of cytoprotective genes through the antioxidant response element (ARE). This endogenous response is one of the major pathways by which cells are protected from xenobiotic or innate oxidative insults. Furthermore, in neural systems, astrocyte-specific activation of Nrf2 is known to protect neurons. In previous work, our laboratory found that Nrf2 protects from intrastriatal injections of the mitochondrial complex II inhibitor malonate. Here, we extend these results to show that multiple methods of astrocyte-specific Nrf2 overexpression provide protection from neurotoxicity *in vivo*. GFAP-Nrf2 transgenic mice are significantly more resistant to malonate lesioning. This outcome is associated with an increased basal resistance, but more so, an enhanced Nrf2 response to lesioning that attenuated the ensuing neurotoxicity. Furthermore, striatal transplantation of neuroprogenitor cells overexpressing Nrf2 that differentiate into astrocytes after grafting also significantly reduced malonate toxicity. Overall, these data establish that enhanced astrocytic Nrf2 response and Nrf2 preconditioning are both sufficient to protect from acute lesions from mitochondrial complex II inhibition.

Key Words: **Nrf2; malonate; astrocyte; neural progenitor cells; neurotoxicity.**

The antioxidant response element (ARE) is a *cis*-acting enhancer sequence found in the promoter region of many detoxification and cytoprotective genes. It was initially identified by Rushmore *et al.* (Rushmore *et al.*, 1991, Rushmore and Pickett, 1990) and is known to be important in the control of a variety of genes in most tissues (Kensler, *et al.*, 2007). Several of the genes known to be regulated in neural tissue are γ-glutamyl cysteine ligase catalytic subunit (GCLC) and modulatory subunit (GCLM), NAD(P)H: quinone oxidoreductase 1 (NQO1), heme-oxygenase 1 (HO-1), and certain glutathione S-transferase (GST) family members. The putative transcription factor that drives ARE-mediated gene expression is nuclear factor E2-related factor 2 (Nrf2) (Itoh, *et al.*, 1997). Nrf2 is a basic leucine zipper transcription factor belonging to the cap "n" collar family. Cytoplasmic repression of Nrf2 activity is dependent on Kelch-like ECH-associated protein 1 (Keap1) (Itoh, *et al.*, 1999), which sequesters Nrf2 in the cytoplasm and also controls its ubiquitin-dependent degradation (Kobayashi, *et al.*, 2004). Upon activation by small molecules, the interaction between Keap1 and Nrf2 is disrupted. Nrf2 protein turnover is thereby attenuated and the transcription factor accumulates and translocates to the nucleus. In the nucleus, Nrf2 binds small Maf proteins and modulates transcription through the ARE (Itoh *et al.*, 1997).

Induction of Nrf2-mediated transcription, particularly in astrocytes, has been shown to protect against neurotoxicity from a variety of insults. In primary neural cultures, Nrf2 activation is known to be neuroprotective against oxidative stressors and mitochondrial toxins, such as the following: hydrogen peroxide, *tert*-butyl hydroperoxide, 6-hydroxydopamine (6-OHDA), 3-nitropropionic acid (3-NP), methylpyridinium ion (MPP^+), and rotenone (Calkins *et al.*, 2005, Jakel *et al.*, 2005, Lee, *et al.*, 2003; Shih *et al.*, 2003, 2005). Furthermore, in whole animals, Nrf2 is known to protect from several models of acute or subchronic neurotoxicity such as malonate, 3-NP, kainic acid, 6-OHDA, methylphenyl-1,2,4,6-tetrahydropyridine (MPTP), and ischemia-reperfusion injury (Burton *et al.*, 2006; Chen *et al.*, 2009; Jakel *et al.*, 2007; Kraft *et al.*, 2006; Satoh *et al.*, 2006, 2008; Shih et al., 2005a, 2005b). Another recent study has demonstrated Nrf2-mediated protection from the chronic motor neuron toxicity associated with dominant mutations in Cu/Zn superoxide dismutase (Vargas *et al.*, 2008). In all cases, either Nrf2 activation was shown to contribute to neuroprotection, or conversely, Nrf2 deficiency led to increased sensitivity. These observations illustrate the critical concept that Nrf2 response is an inducible and highly protective mechanism that may be employed by cells in culture or *in vivo* to combat oxidative toxicity.

Mitochondrial complex II inhibitors, malonate and 3-NP, have been used to induce striatal medium spiny neuron

degeneration that is highly reminiscent of Huntington's disease (Beal *et al*., 1993a, 1993b; Brouillet, *et al*., 1993). Because they are relatively acute models that do not require breeding of transgenic mice, they are well suited to address questions about the protective mechanism of Nrf2 or to evaluate the potential of therapeutic strategies that require Nrf2 activation. Previously, it was shown that Nrf2-deficient mice are more susceptible to both malonate and 3-NP toxicity (Calkins, *et al*., 2005, Shih, *et al*., 2005) and that grafting of Nrf2-overexpressing astrocytes could protect from malonate lesioning (Calkins, *et al*., 2005). In order to expand this work and better understand the underlying mechanisms of protection by astrocytic Nrf2 overexpression, striatal lesions were induced with malonate in a genetic model of astrocyte-specific Nrf2 overexpression. Furthermore, Nrf2-overexpressing mouse neuroprogenitor cells (NPCs) were transplanted into the striatum. The vast majority of grafted NPCs differentiates into astrocytes and provides evidence in support of a clinically relevant method for *ex vivo* gene therapy. Using these two methods, we clearly demonstrate that astrocyte-specific Nrf2 overexpression confers dramatic neuroprotection against malonate lesioning. Additionally, the data distinguish between enhanced Nrf2 activation prior to insult versus enhanced Nrf2 activation during the pathogenic process. We conclude that Nrf2 activation prior to insult and increased Nrf2 response concurrent with pathological development are both sufficient to limit striatal damage from mitochondrial complex II inhibition.

MATERIALS AND METHODS

Animals. ARE-hPAP transgenic and GFAP-Nrf2 transgenic mice were bred separately on a BL6/SJL background. ARE-hPAP mice were created by insertion of a 51-bp segment of the promoter from rat *NQO1* gene, which contains the core ARE sequence, upstream of a minimal promoter and the gene for the heat stable human placental alkaline phosphatase (hPAP) (Johnson, *et al*., 2002). GFAP-Nrf2 mice (Vargas, *et al*., 2008) were created by insertion of the mouse *Nrf2* gene downstream of the gfa2 promoter, a 2.2-kb segment of the human glial fibrillary acidic protein (GFAP) promoter (Brenner and Messing, 1996). All experiments were approved by and performed according to the ethical guidelines provided by the Animal Care and Use Committee at the University of Wisconsin Medical School.

Real-time PCR. Isolation of mRNA was performed using TRIZOL according to the manufacturer's instructions (Invitrogen). Quality and concentration of mRNA were measured using the Agilent 2100 Bioanalyzer. Reverse transcriptase reactions were run on 1 μg of total mRNA using the Reverse Transcription System (Promega). Quantitative PCR was performed using a Light Cycler 480 (Roche) and the SYBR Green I Master (Roche) according to manufacturer's instructions. Primer sequences for actin, GFAP, Nrf2, NQO1, HO-1, GCLM, and GCLC were published previously (Vargas *et al*., 2008). Additional primer sequences are as follows: Keap1, AAG GAC CTT GTG GAA GAC CA and CCC TGT CCA CTG GAA TTG AT, and Iba-1, GGA TTT GCA GGG AGG AAA AG and TGG GAT CAT CGA GGA ATT G. Primer sequences for NADPH oxidase subunits p91phox and p67phox, as well as Mac-1 were taken from Wu *et al*. (2003).

Western blot. Striatal tissue was homogenized in 1% SDS buffer and boiled for 5 min. Small aliquots of the extracts were retained for protein determination by the BCA assay kit (Pierce) with bovine serum albumin (BSA) as the standard. Equal amounts of protein (20 μg) were separated by SDS-polyacrylamide gel electrophoresis (10% polyacrylamide gels) and transferred onto the polyvinylidene fluoride membranes (Millipore, Bedford, MA). Membranes were blocked overnight at 4°C in 5% milk, 5% BSA in Tris-buffered saline plus 0.1% Tween-20 (TBST) buffer. Blots were then incubated for 2 h at room temperature with blocking solution containing the primary antibody. The goat polyclonal antibody against NQO1 (1:1000) was purchased from Abcam. The polyclonal antibodies against GCLC and GCLM (1:20,000 dilution for each) were kind gifts from Dr Terrence Kavanaugh (University of Washington, Seattle, WA). The GST A4 polyclonal antibody (lot number 940126, 1:2,000 dilution) was a kind gift from Dr John D. Hayes (University of Dundee, Dundee City, Scotland, UK). The anti-β-actin serum (1:20,000 dilution) was from Sigma Co. (St Louis, MO). After 3× 10-min washes in TBST buffer, blots were incubated for 1 h at room temperature with horseradish peroxidase–conjugated secondary antibodies in blocking solution: 1:2,000 goat anti-rabbit IgG (Amersham Pharmacia Biotech, Piscataway, NJ). Finally, the blots were washed 3× 10 min in TBST and developed using the enhanced chemiluminescence (ECL) procedure of Amersham Pharmacia Biotech. The signals were exposed with Hyperfilm (Amersham Pharmacia Biotech), and the blots were stripped and reprobed with anti-β-actin antibodies as a quantitative control. The resulting gel bands were scanned and quantified using ImageJ. Band intensity was normalized to β-actin.

hPAP activity. Activity of the hPAP reporter was measured as previously described (Johnson *et al*., 2002; Vargas *et al*., 2008). Briefly, cells were lysed in TMN (50mM Tris, 5mM $MgCl_2$, 100mM NaCl) with 1% 3-[(3-cholamidopropyl)dimethylammonio]-1-propanesulfonate (CHAPS) by a single freeze thaw cycle. Tissues were homogenized in TMN with 4% CHAPS with a tissue homogenizer (IKA) at approximately 1–10 mg wet weight per milliliter. An aliquot of the lysate was added to 0.2M diethanolamine and heated to 65°C for 20–30 min to inactivate endogenous alkaline phosphatase activity. After heat inactivation, CSPD and Emerald (Applied Biosystems) were used as luminescent substrate and enhancer, respectively. Luminescence was measured in 96-well plates with a Berthold luminometer and corrected for soluble protein. Cell cultures were visually inspected for health and similar cell numbers prior to lysis.

hPAP histochemistry. Histochemistry for the hPAP reporter was performed as previously described for cultured cells (Johnson *et al*., 2002) with minor modifications to allow for tissue staining (Calkins, *et al*., 2005, Jakel, *et al*., 2005). Animals were sacrificed with CO_2 and then transcardially perfused first with PBS followed by 4% paraformaldehyde in PBS. Perfused animals were set aside for 5 min and then brains were removed into PBS at 4°C overnight. Tissue was cryoprotected with 30% sucrose in PBS and then embedded in Optimal Cutting Temperature. Slides were prepared with PFA-fixed tissue from hPAP transgenic or wild-type control tissue and rehydrated in TMN for 10 min. Slides were incubated at 65°C in preheated TMN for 20 min, cooled and then removed to either TMN with 5-bromo-4-chloro-3-indolyl phosphate/nitro blue tetrazolium at 37°C or else Vector Red substrate in the provided buffer (Vector Labs). Color development was monitored and samples were counterstained and coverslipped as appropriate.

Glutathione measurement. Total glutathione levels (reduced glutathione [GSH] and oxidized glutathione [GSSG]) were determined using the method developed by Tietze (1969). Briefly, dithionitrobenzoic acid (DTNB) reduction by GSH was monitored spectrophotometrically. This reaction produces GSSG which can be recycled to GSH using glutathione reductase (GSSG Rdx) and NADPH. Conditions are set such that total GSH in the reaction is rate limiting. Cell culture or dissected tissue samples were harvested and flash frozen. All samples were homogenized with an IKA tissue homogenizer for 20 s in ice-cold 3% perchloric acid and centrifuged at 4°C at 7400 × g. The supernatant was diluted 10-fold with 0.1M Na_2HPO_4, and pellets were reserved. Precipitated protein was resolublized in 1% SDS and concentration was measured by the BCA method (Pierce). The neutralized supernatant was transferred into 96-well plates containing 0.1M potassium phosphate buffer

(pH 7.5) with 0.1 mg/ml DTNB and 0.32 mg/ml NADPH. Using a visible spectrum 96-well plate reader, total glutathione was assayed by the change in absorbance at 405 nm. The reaction was started by the addition of 8 units/ml GSSG Rdx (Calbiochem). Total glutathione concentrations were determined from standard curves and then standardized to sample protein.

Neural progenitor cell cultures. NPCs were cultured from mouse embryos as suspended neurospheres by methods previously described with minor modifications (Li, *et al*., 2005; Rietze and Reynolds, 2006). Briefly, striatal tissue was dissected into ice-cold Hank's balanced salt solution without Ca^{++} or Mg^{++} (HBSS) from E14 mouse embryos derived from ARE-hPAP transgenic hemizygous males crossed with wild-type females. Trypsin was added at a final concentration of 0.1% and tissue was incubated at 37°C for 10 min. Tissue was centrifuged and washed three times with HBSS and finally triturated into a single-cell suspension in growth media. Cells were maintained at 37°C in normoxic conditions (5% CO_2 and 5% O_2) environment in 30% F-12 (Hams) and 70% Dulbecco's Modified Eagle Medium (DMEM) with B27 supplement and 20 ng/ml epidermal growth factor (EGF). Half media changes were made every 3 days, at which point EGF was replenished.

For plating experiments, spheres that had been cultured for at least 2 weeks were allowed to settle and incubated with Accutase for 15 min at 37°C. After dissociation by trituration, cells were plated onto poly-D-lysine–coated plastic dishes and maintained in growth media without EGF. Under these conditions, regardless of Nrf2 overexpression, cells differentiated into approximately 73% astrocytes, 22% neurons, and 5% oligodendrocytes (data not shown).

Adenovirus infection. Adenoviral infection of cells was performed 48 h prior to differentiation or 24 h prior to transplantation at a multiplicity of infection (MOI) of 50 pfu/cell. Cell number was estimated using a small aliquot from the well-mixed culture that was triturated to a single-cell suspension. Virus was added directly to culture media, and spheres were incubated for 24 or 48 h after which they were washed with growth media three times.

Intrastriatal stereotaxic injections. Mice were anesthetized with vaporized isofluorane and placed in a stereotaxic frame, with an attached motorized programmable injector (Stoelting). After exposing the skull, bregma was located and small holes were drilled through the skull 0.5 mm anterior and 2.1 mm lateral to the midline in both directions. Injections were made 3.3 mm ventral to dura using a 33G stainless steel blunt tipped needle (Hamilton). All injections were performed over the course of 5 min (0.2 μl/min), and the needle was held in place for 5 min prior to withdrawal.

NPC grafting. NPC cultures that were infected 24 h prior were washed three times with growth media and then once with DMEM. Neurospheres were allowed to settle by gravity and then excess DMEM was removed leaving a slurry from which injections were made. At the time of infection, neurospheres were visually inspected for uniform spherical shape and approximately 100–200 μm diameter. The density of cells at time of injection was routinely between 20,000 and 50,000 cells/μl, with individual spheres composed of approximately 5,000–10,000 cells. Three to five spheres were loaded into the syringe for each injection in a volume of 1 μl.

Malonate injections. Mice received malonate lesions by intrastriatal stereotaxic injection with contralateral vehicle injections. Malonate (0.5 μmol/1 μl or 0.75 μmol/1 μl, pH 7.4, in 0.9% NaCl) was injected 0.5 mm anterior to bregma, 2.1 mm lateral to midline, and 3.3 mm ventral to dura. In the case where NPCs were previously injected, new measurements were taken for the second injection. All new measurements coincided with the earlier injection sites.

Histological analysis. Animals were euthanized with CO_2 and transcardially perfused with PBS followed by 4% PFA. After approximately 5 min, brains were removed to PBS and stored at 4°C overnight. Fixed tissue was then transferred to 30% sucrose for cryoprotection, after which it was frozen and sectioned at 40 μm on a cryostat (Leica). Sections taken every 0.2 mm were stained with cresyl violet to visualize lesions. Lesion area for each section was calculated using Zeiss Axiovision software and lesion volume was estimated by multiplying the individual lesion areas by the distance between sampled sections.

Immunohistochemistry. Immunohistochemistry was performed using standard methods for frozen tissue. Monoclonal anti-GFAP (clone 2A5) antibody (Sigma) was used at 1:1000 dilution. Secondary antibodies were Texas-Red anti-mouse (Vector Labs) or fluorescein isothiocyanate anti-mouse (Vector Labs). Both were used at 1:200 dilution.

Statistics. *In vivo* experiments were performed on mice with littermate controls populating all groups. Most statistical comparisons were made between parametric data using Student's *t*-test. Multivariate data were analyzed using two-way ANOVA with Bonferroni posttest. In all cases, statistical significance was set at $p < 0.05$. Data are presented as mean ± SEM.

RESULTS

GFAP-Nrf2 Transgenic Mice Are Resistant to Malonate Lesioning but Do Not Exhibit Qualitatively Different Pathologic Response

GFAP-Nrf2 transgenic and wild-type littermates were intrastriatally injected with 0.5M malonate and sacrificed after 48 h. Sections were sampled every 0.2 mm and stained with cresyl violet for lesion volume analysis (Fig. 1A). Quantification (Fig. 1B) showed that lesions in the wild-type mice were larger than those in the GFAP-Nrf2 mice (wild type, 2.81 ± 1.09 vs. GFAP-Nrf2, 0.68 ± 0.26 mm^3). However, there was no observable qualitative difference in the lesions between genotypes. All lesions exhibited degenerating cells in the lesion area as visualized by cresyl violet, with GFAP and Iba-1 immunoreactivity in the penumbra. GFAP immunoreactivity is indicative of reactive astrogliosis and is a typical response to neurological damage. Iba-1 immunoreactivity occurs as a result of microglial activation and also is a stereotypical response to damage. Not only were there no observable differences in relative amount of GFAP or Iba-1 signal, but cell morphology was similar as well (Fig. 1C). This was true for both reactive astrocytes and reactive microglia.

In order to further probe the astrocyte and microglial response, qPCR for striatal GFAP, Iba-1, Mac-1, and two subunits of NADPH-oxidase was performed in a time course after malonate injection (Fig. 2). NADPH oxidase subunits and Mac-1 are expressed in all types of macrophage cells, and appearance of these indicates either microglial presence or infiltration of monocytes from the periphery. The transcriptional response occurred as expected over the course of 1 week. GFAP expression was elevated at the earliest measured time point (24 h), while Iba-1 and macrophage markers increased steadily up to 7 days. Genotype did not affect the expression of any of the genes observed. GFAP appeared to be decreased in malonate lesioned hemispheres of GFAP-Nrf2 mice compared to wild type at the 48 h and 7-day time points; however, statistical significance was not achieved. This observation can be explained by the smaller volume of lesions in the GFAP-Nrf2

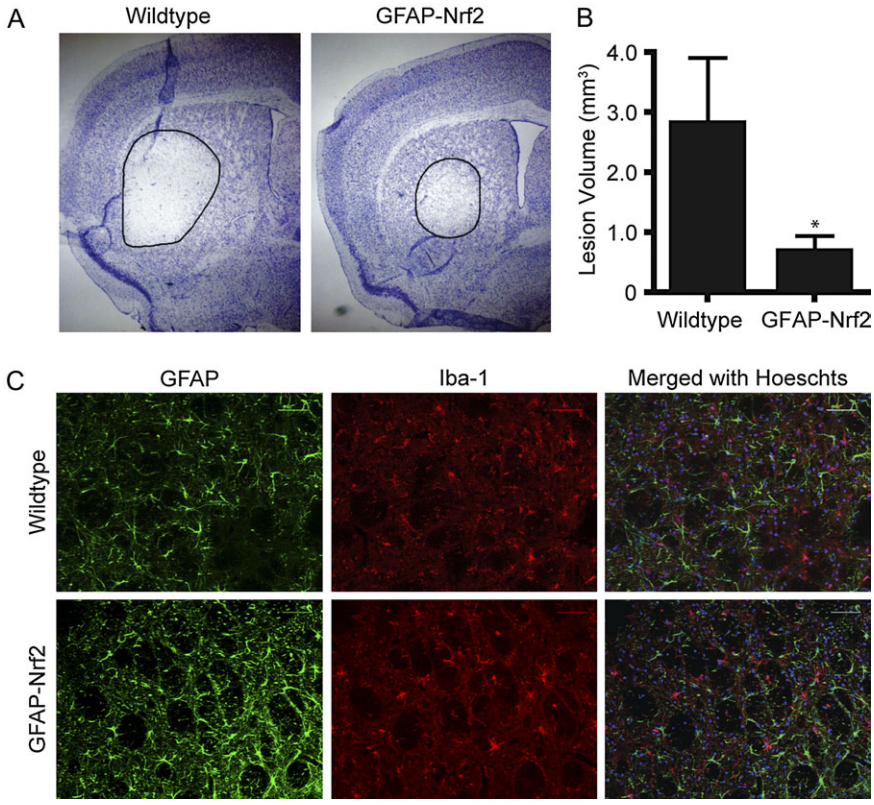

FIG. 1. GFAP-Nrf2 transgenic mice are resistant to malonate lesions but exhibit similar reactive gliosis. Mice were unilaterally injected with 0.5 μmol malonate and sacrificed after 48 h (wild type: $n = 8$, GFAP-Nrf2: $n = 6$). (A) Representative lesions are visualized by cresyl violet staining. (B) Quantification of lesion volume in GFAP-Nrf2 transgenic mice and wild-type littermate control animals. (C) GFAP (green) and Iba-1 (red) immunoreactivity in the penumbra of the lesion is similar in both GFAP-Nrf2 and wild-type mice. *$p < 0.05$ compared with wild-type animals.

mice. Smaller lesion volumes would lead to smaller penumbral areas, which should in turn be reflected by less GFAP.

GFAP-Nrf2 Transgenic Mice Do Not Exhibit Major Differences from Wild Type in Cortex or Striatum under Basal Conditions

In order to test whether basal differences in striatal tissue from the GFAP-Nrf2 transgenic mice contribute to the observed neuroprotection, expression of Nrf2, GFAP, Keap1, and several genes known to be regulated by Nrf2 was measured. Expectedly, Nrf2 mRNA was increased nearly fourfold in the GFAP-Nrf2 mice compared to wild type (Fig. 3A). Keap1 mRNA was measured to determine whether Nrf2 overexpression would feed back to influence expression of this central regulator of Nrf2 activity. No expression differences were found for Keap1 in striatum. Furthermore, the expression of several known Nrf2-driven genes including NQO1, GCLM, GCLC, and HO-1 were evaluated. Statistically significant increases in gene expression were seen only for NQO1, while expression of the other measured genes showed trends toward an increase.

Protein levels of Nrf2-regulated genes, NQO1, GCLM, and GCLC (Fig. 3B), in both striatum and cortex were also determined. According to Western blot analysis, no protein increases were present in the GFAP-Nrf2 striatum or cortex. However, reporter gene activity of ARE-hPAP mice crossed with the GFAP-Nrf2 transgenic mice (Fig. 3C) showed several fold increases in hPAP reporter activity (striatum; 20.3-fold increase, cortex; 5.4-fold increase) in GFAP-Nrf2(+)/ARE-hPAP(+) compared to GFAP-Nrf2(−)/ARE-hPAP(+) mice. Because this reporter construct is specifically designed to measure Nrf2 activation, it is probably not subject to any compensatory regulation and will reflect only Nrf2 activity. Finally, glutathione (GSH) levels were not significantly increased in either tissue (Fig. 3D). The lack of measurable increases in most mRNA, protein, and GSH levels indicates that while Nrf2 expression is increased, there is no apparent change in Nrf2-dependent outcomes measured in either cortex or striatum under basal conditions.

Activation of Astrocyte Nrf2 Signaling Is Enhanced after Malonate Lesioning in GFAP-Nrf2 Mice

Because there were no major differences in Nrf2-dependent targets in the basal condition of GFAP-Nrf2 mice (Fig. 3), we hypothesized that protection from malonate lesioning occurs as a result of enhanced Nrf2 activation in this transgenic line. Therefore, expected gene expression changes in Nrf2 and Nrf2

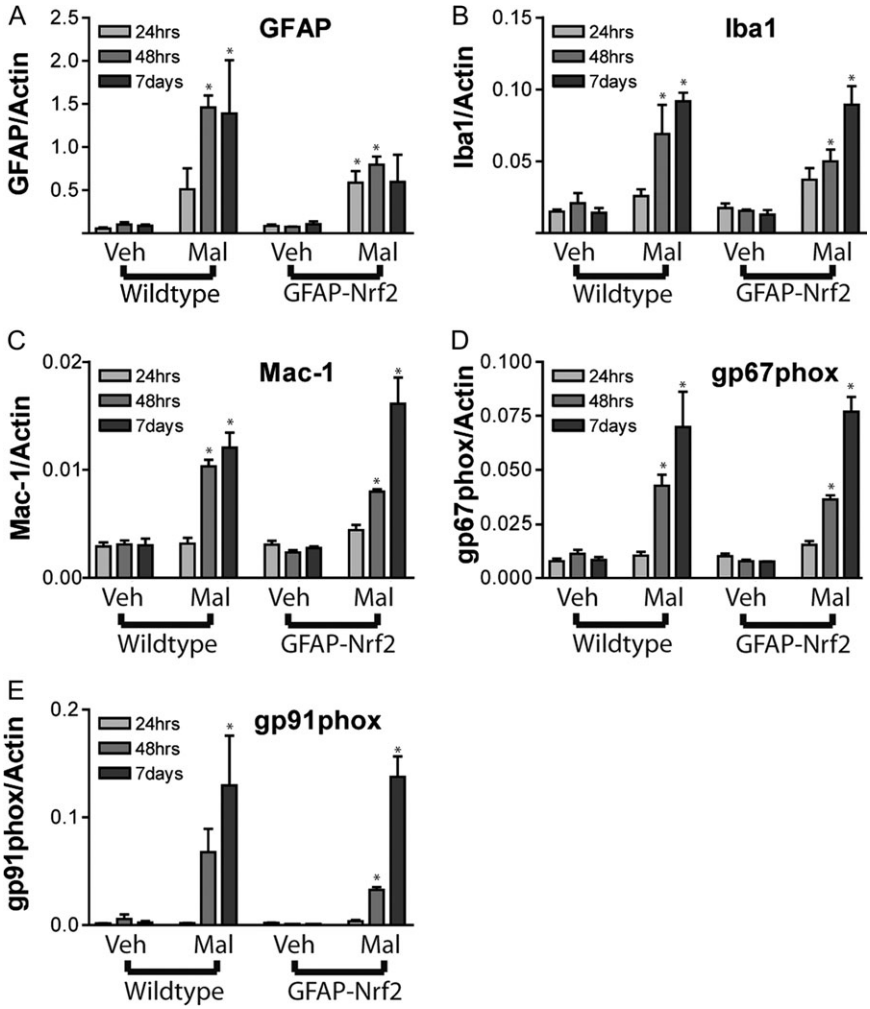

FIG. 2. GFAP-Nrf2 exhibit similar induction of mRNA related to gliosis or immune response. Mice injected with 0.5 μmol malonate were sacrificed 24 h, 48 h, or 7 days after lesioning and mRNA levels were evaluated for (A) GFAP, (B) Iba-1, (C) Mac-1, (D) gp67phox, and (E) gp91phox ($n = 3$–5 mice per group). No statistically significant genotype effect was found for any gene. Time had a significant effect in all genes except GFAP ($p < 0.05$). Malonate treatment produced statistically significant effects in all genes. *$p < 0.05$ compared with vehicle hemisphere by Bonferroni posttest. #$p < 0.05$ compared with wild-type animals by Bonferroni posttest.

target genes were determined at 24 h, 48 h, and 7 days after lesioning. In wild-type mice, malonate lesioning produced significant changes in total striatum expression of Nrf2 at 7 days (Fig. 4A). Similar changes in HO-1 were also observed at 48 h and 7 days (Fig. 4D). In contrast, NQO1 and GCLM did not increase (Figs. 4B and 4C). As described in Figure 3, the GFAP-Nrf2 mice had increased basal levels of expression of Nrf2 without significant changes in Nrf2-dependent genes (Fig. 4). However, the transgenic mice respond differently to the lesioning. Maximum Nrf2 expression levels were seen at 24 h in the lesion hemispheres of GFAP-Nrf2 mice compared to wild-type mice (Fig. 4A) and returned to normal expression levels by 7 days (Fig. 4A). Unlike the wild-type mice, Nrf2-driven genes, NQO1, GCLM, and HO-1, mirrored this pattern of increased expression almost exactly in the GFAP-Nrf2 mice (Figs. 4B–D). This more rapid response to the lesioning and the greater increase in gene expression in GFAP-Nrf2 mice suggests that these mice have an enhanced ability to attenuate lesion propagation compared to the wild type.

ARE-hPAP Reporter Activity Is Robustly Increased after Malonate Lesioning Coincident with Reactive Astrocytes

In order to confirm that the enhanced Nrf2 response in GFAP-Nrf2 mice occurs in astrocytes, GFAP-Nrf2 mice were crossed with ARE-hPAP reporter mice and lesioned with malonate. Mice were sacrificed 48 h after lesioning and brain was harvested either by dissection and flash freezing for hPAP activity or else soft fixed by transcardial perfusion for histochemical analysis of hPAP activity. Histochemical stains of the tissue revealed that the majority of increased reporter activity coincides with the ring of activated astrocytes and microglia that typically forms in the penumbra of the lesion.

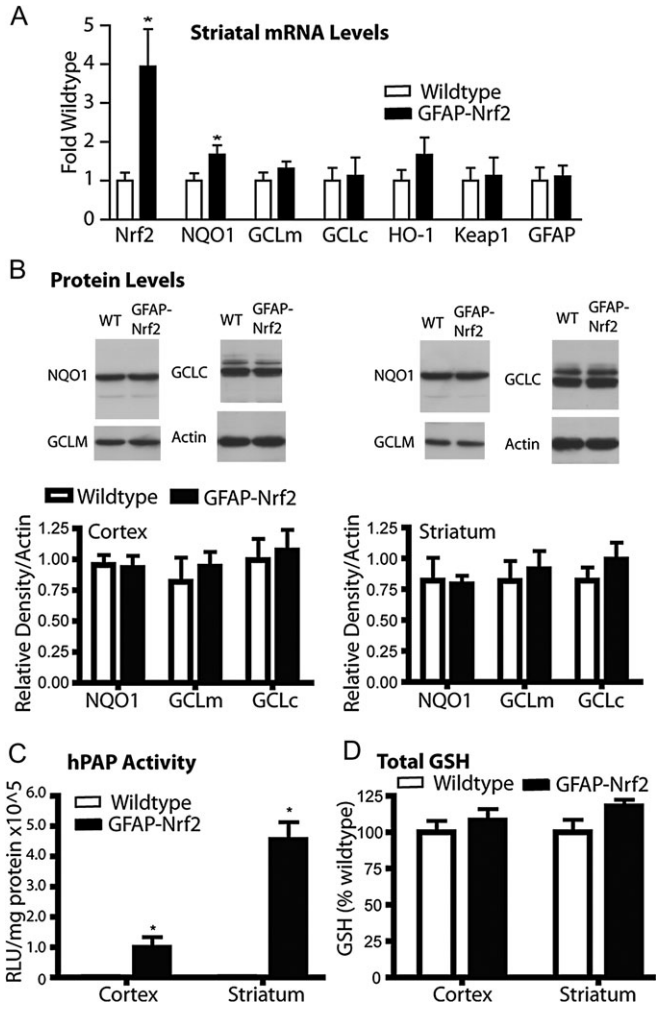

FIG. 3. Cortical and striatal tissue from GFAP-Nrf2 transgenic mice shows only minor differences from wild-type mice. (A) Quantitative PCR for Nrf2-, GFAP-, Keap1-, and Nrf2-driven genes was performed on striatal tissue from wild-type and GFAP-Nrf2 transgenic mice. Data were normalized first to actin expression from the same tissue and then to wild type ($n = 4$ wild type, $n = 4$ GFAP-Nrf2). (B) Western blot analysis was performed to measure protein levels of Nrf2-driven genes in cortex and striatum. Data are normalized to actin ($n = 4$ wild type, $n = 4$ GFAP-Nrf2). (C) Activity for the ARE-hPAP reporter protein was measured in GFAP-Nrf2 transgenic, ARE-hPAP reporter mice as well as ARE-hPAP reporter mice alone. Data are normalized to protein and then background levels determined from ARE-hPAP–negative mice are subtracted ($n = 3$ wild type, $n = 3$ GFAP-Nrf2). (D) Total glutathione levels in cortex and striatum of GFAP-Nrf2 transgenic or wild-type mice were determined, normalized to protein, and then normalized to wild type values ($n = 4$ wild type, $n = 4$ GFAP-Nrf2). $^{*}p < 0.05$ compared to GFAP-Nrf2 nontransgenic.

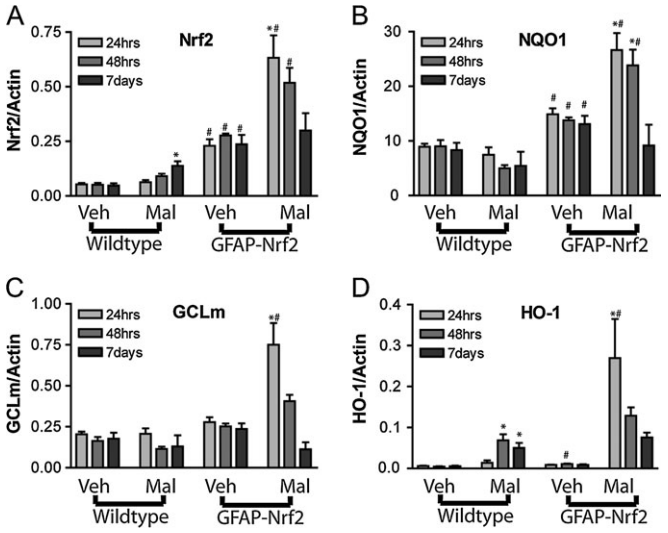

FIG. 4. GFAP-Nrf2 exhibit enhanced induction of Nrf2 and Nrf2-driven genes mRNA in response to malonate lesioning. Mice injected with 0.5 μmol malonate were sacrificed 24 h, 48 h, or 7 days after lesioning and mRNA levels were evaluated for (A) Nrf2, (B) NQO1, (C) GCLM, and (D) HO-1 ($n = 3$ to 5 mice per group). Malonate-treated animals held statistically significant differences attributed to genotype for all genes ($p < 0.05$). Statistically significant time effects were found for NQO1 and GCLM only. Treatment effects were also found for all genes ($p < 0.05$). $^{*}p < 0.05$ compared with vehicle hemisphere by Bonferroni posttest. $^{\#}p < 0.05$ compared with wild-type animals by Bonferroni posttest.

In GFAP-Nrf2(−)/ARE-hPAP(+) mice, previous observations (Calkins, *et al.*, 2005) were confirmed that reporter activity is increased in this area as well (Fig. 5A, left panel). The intensity of staining and number of cells that stain positively are noticeably different in the GFAP-Nrf2(+)/ARE-hPAP(+) mice (Fig. 5A, right panel). Furthermore, this increased staining is coincident with GFAP immunoreactivity in the lesion penumbra (Fig. 5B). Quantification of hPAP activity produced results that reflect the previous mRNA measurements, reflecting the dramatically increased Nrf2-driven gene expression in response to lesioning in the GFAP-Nrf2 mice (Fig. 5C). Malonate exposure in the GFAP-Nrf2(+)/ARE-hPAP(+) mice led to a significant increase in hPAP activity of 53,200 RLU/μg protein compared to vehicle, whereas a small but nonsignificant increase in hPAP activity of 402 RLU/μg protein was observed following malonate exposure in GFAP-Nrf2(−)/ARE-hPAP(+) mice. Finally, the significant changes noted in the expression of a key glutathione synthesis gene (GCLM; Fig. 4C) following malonate exposure in GFAP-Nrf2 mice did indeed lead to increased GSH in tissue (Fig. 5D). In fact, GFAP-Nrf2 mice have almost 44% more glutathione after malonate lesioning than the wild type. It is notable that the wild-type mice have similar levels of striatal glutathione after vehicle or malonate treatment and also that the GSH difference in GFAP-Nrf2 mice after vehicle and malonate treatment did not reach statistical significance.

Nrf2-Overexpressing NPC Cultures Exhibit Substantial Changes in Factors Known to Influence Antioxidant Status

NPC cultures were prepared from individual ARE-hPAP transgenic or nontransgenic cortical tissue and grown for at least 2 weeks. Cells were infected with either 50 MOI Ad-GFP or 50 MOI Ad-Nrf2. After 48 h, one half of the cells were plated for differentiation. The rest of the culture was harvested

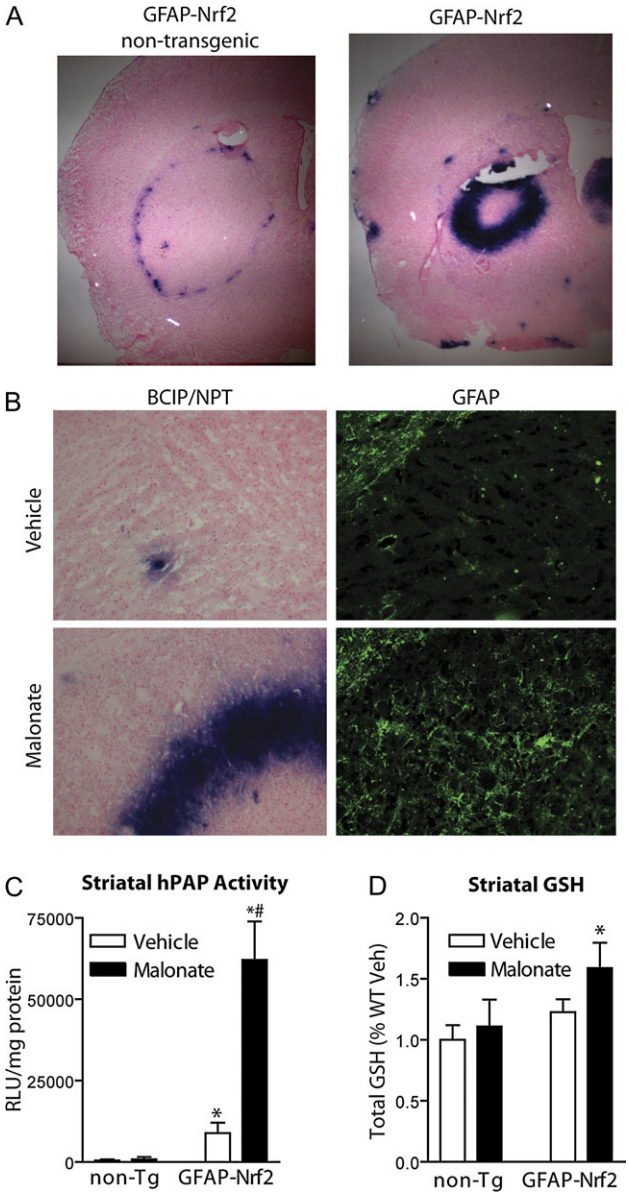

FIG. 5. GFAP-Nrf2 transgenic mice respond to malonate lesioning with enhanced Nrf2 activation in the lesion penumbra. ARE-hPAP(+) transgenic mice and GFAP-Nrf2(+)/ARE-hPAP(+) double-transgenic mice were lesioned with malonate and sacrificed after 48 h for (A) histochemical evaluation of the hPAP activity. (B) Serial sections were stained histochemically for hPAP activity and immunohistochemically for GFAP. Pictures were taken with the corpus callosum visible in the upper left-hand corner of each panel. (C) Striatal hPAP activity was measured 48 h after lesioning nontransgenic wild-type and GFAP-Nrf2 mice ($n = 3$ in all groups). (D) Total tissue GSH was measured 24 h after malonate injection ($n = 4$ in all groups). $^{*}p < 0.05$ compared to GFAP-Nrf2 nontransgenic. $^{\#}p < 0.05$ compared to noninjected hemispheres.

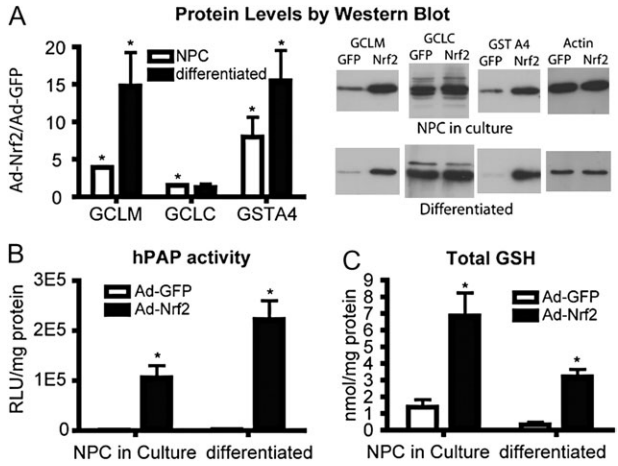

FIG. 6. Ad-Nrf2–infected NPCs exhibit robust increases in expected Nrf2-mediated response. (A) Western blot analysis was performed to measure protein levels of Nrf2-driven genes in Ad-GFP– and Ad-Nrf2–infected neurospheres and differentiated cultures. Data were normalized first to actin expression from the same sample and then to Ad-GFP–infected cells ($n = 4$). (B) Activity for the ARE-hPAP reporter protein were measured in cells derived from ARE-hPAP reporter mice and infected with Ad-GFP or Ad-Nrf2. Data are normalized to protein and then background levels determined from ARE-hPAP–negative cultures are subtracted ($n = 4$). (C) Total glutathione levels in neurosphere cultures or differentiated cells that were infected with either Ad-GFP or Ad-Nrf2 ($n = 4$). All data represent at least four cultures derived from separate individual pups. $^{*}p < 0.05$ compared to Ad-GFP–infected cells.

(NPC in culture). Differentiated cells were harvested 3 days after plating (5 days after infection). Protein levels of several Nrf2-driven genes (Fig. 6A) were measured. GCLM and GSTA4 protein levels were significantly increased in both NPC in culture and differentiated cultures. Additionally, hPAP activity after infection was measured in ARE-hPAP transgenic cells, and increased hPAP activity was observed under both conditions (Fig. 6B). Total GSH was also measured. NPC and differentiated cultures both exhibited greater GSH levels after Ad-Nrf2 infection compared with Ad-GFP–infected cells (Fig. 6C). Overall, these data show that Ad-Nrf2 infection of NPC leads to massive increases in expected mRNA expression, protein levels, and GSH. Importantly, these effects persist through the process of differentiation, making the cells suitable for use in grafting experiments.

Ad-Nrf2 Transduced NPC Protect from Malonate Lesions Compared to Ad-GFP–Transduced NPC

Mice that were at least 8 weeks old were grafted bilaterally with NPCs that had been previously transduced with either Ad-GFP or Ad-Nrf2. Two weeks after grafting, mice were sacrificed to assess survival and functionality of the grafts. Wild-type mice were grafted with ARE-hPAP reporter cells, and brain was sectioned and stained for hPAP histochemsitry. A small number of Ad-GFP–infected cells stained positively for the hPAP reporter, but overall, Nrf2 activation was limited to the Ad-Nrf2–infected cells (Fig. 7A). Grafted cells typically remained near the injection site and migrated less than 1 mm from the original needle tract. Survival and integrity of the grafts was assessed by GFP expression and no apparent difference was observed between Ad-GFP cells and Ad-Nrf2 cells (data not shown). The identity of the GFP-overexpressing

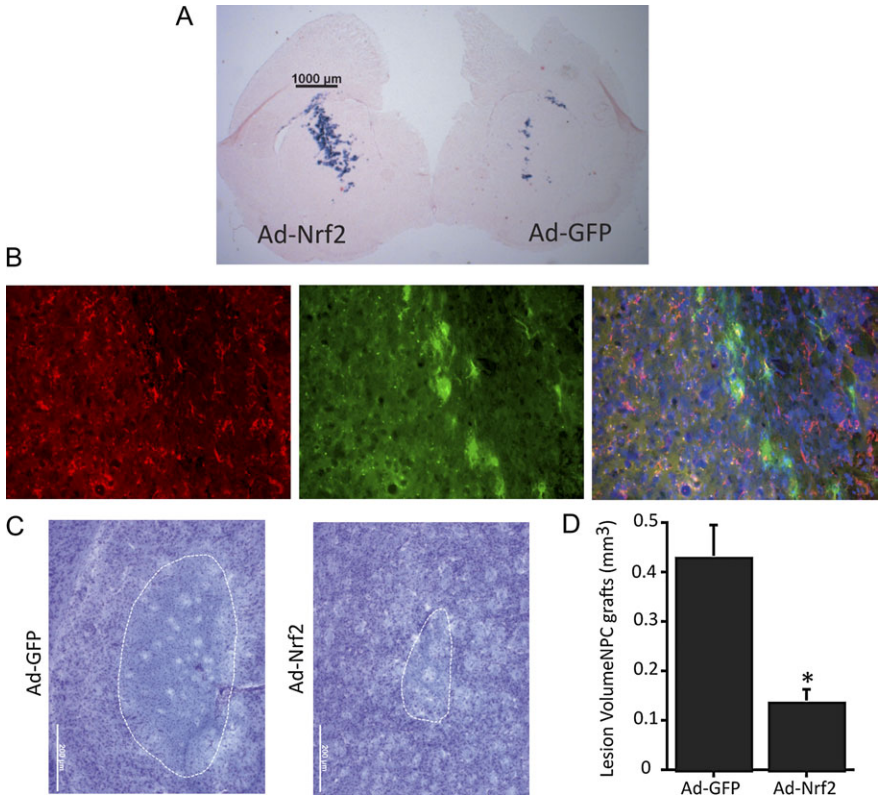

FIG. 7. Nrf2 overexpressing NPC differentiate into astrocytes and protect from malonate lesioning. ARE-hPAP transgenic NPC infected with Ad-GFP were grafted into wild-type striatum. Ad-Nrf2–infected NPC were grafted into the contralateral striatum. Mice were sacrificed for evaluation of grafts 2 weeks postsurgery or lesioned with malonate. Lesioned animals were sacrificed after 48 h. (A) Histochemistry was performed for the ARE-hPAP reporter on sections containing both Ad-GFP– and Ad-Nrf2–grafted cells. (B) GFP-positive cells colabeled for GFAP, indicating an astrocytic identity. (C) Representative maximal lesion areas are shown for Ad-GFP–grafted hemispheres and Ad-Nrf2–grafted hemispheres. (D) Quantification of graft volume was performed on cresyl violet–stained sections throughout the striatum ($n = 4, 4$). *$p < 0.05$ compared to hemispheres receiving Ad-GFP–transduced cells.

cells was probed with immunohistochemical staining of astrocyte and neuronal markers (GFAP and β-III-tubulin, respectively). GFP colocalized exclusively with GFAP (Fig. 7B). Not all the GFP-positive cells colocalized with either stain, but none colocalized with β-III-tubulin (data not shown). Many astrocytes do not express immunohistochemically detectable levels of GFAP under normal conditions, so it is unsurprising that we did not observe complete colocalization of GFP cells with GFAP.

Mice were grafted bilaterally with either Ad-GFP– or Ad-Nrf2–transduced NPC (between 20,000 and 50,000 cells/injection). After 4 weeks, they were lesioned with malonate and sacrificed 48 h after lesioning. Representative pictures of striatal lesions are shown (Fig. 7C). Quantification of lesion volume showed significant protection by the Ad-Nrf2 NPC grafts compared to Ad-GFP NPC grafts (Fig. 7D).

DISCUSSION

The data presented herein clearly demonstrate the importance of an astrocytic Nrf2-mediated response to malonate exposure in mitigating subsequent propagation of damage. This response is dramatically enhanced in transgenic mice engineered to overexpress Nrf2 in astrocytes. Interestingly, baseline differences in Nrf2-dependent parameters between GFAP-Nrf2 and wild-type animals are not robust and are unlikely to explain the observed resistance. In addition, the glial response to toxicity does not appear to be altered in GFAP-Nrf2 mice since both wild-type and GFAP-Nrf2 mice show high similarity in both cell density and morphology within the penumbra. We hypothesize that this increased responsiveness provides protection from neurodegeneration after initiation of the pathogenic process. In support of this concept, the penumbra in GFAP-Nrf2 mice exhibit a more pronounced Nrf2 activation at the penumbra boundary as measured in the ARE-hPAP reporter mouse. These observations are in accordance with previous findings that demonstrate GFAP-Nrf2 mice are resistant to MPTP toxicity (Chen, *et al.*, 2009). In that study, slight increases (10–20%) in Nrf2-dependent genes were noted in the striatum and substantia nigra of GFAP-Nrf2 mice. Exposure of these mice to MPTP generated a similar enhanced Nrf2 activation in both regions after treatment with MPTP relative to wild-type controls. Thus, increased resistance to malonate as

well as MPTP is most likely due to an enhanced Nrf2 responsiveness in GFAP-Nrf2 mice.

In contrast to these data from the cortex, striatum, and substantia nigra, the GFAP-Nrf2 mice exhibit increased baseline Nrf2-dependent changes in spinal cord (Vargas, *et al*., 2008). The difference between spinal cord and brain tissue may be at least partially due to baseline GFAP expression levels. After crossing the GFAP-Nrf2 mice with ARE-hPAP reporter mice, histochemically measurable hPAP reporter activity is nearly exclusively restricted to cells that also exhibit GFAP immunoreactivity. It is widely accepted that most astrocytes do not exhibit GFAP immunoreactivity under basal conditions. Similarly, we do not observe detectable histochemical hPAP activity in most astrocytes. However, after a toxic event, GFAP immunoreactivity is dramatically increased. Coincident with this increase, hPAP activity increases as well.

The lack of robust Nrf2-dependent changes in the basal condition of GFAP-Nrf2 mice striatum and cortex might be explained in two ways. First it may be that the GFAP promoter, under basal conditions, does not produce enough Nrf2 message and subsequent protein to effectively overcome negative regulation by Keap1. Under this scenario, we would expect to observe increased GFAP message level coincident with increased Nrf2 message level during astrogliosis. These increases in message would potentially lead to enough translated Nrf2 protein to overcome the threshold of Keap1 negative regulation without disruption of the Keap1-Nrf2 complex. Therefore, the GFAP-Nrf2 construct would produce Nrf2-ARE signaling in much the same way as adenoviral Nrf2 overexpression. The second potential explanation would be that increased Nrf2 protein is indeed negatively regulated by Keap1, but under Nrf2 activating conditions, the excess protein is able to mount an increased response, leading to significantly increased transcript levels of Nrf2-driven genes. The data in this article do not clearly address the question of which mechanism leads to increased Nrf2 response in GFAP-Nrf2 mice. It is likely that both mechanisms will contribute to the enhanced Nrf2-ARE response. Certainly, Nrf2-dependent changes become quite pronounced after toxin administration. Therefore, the GFAP-Nrf2 transgenic mouse model can be considered a good tool for modeling enhanced astrocyte-Nrf2 response to striatal toxicity.

In this article, we also use this protective strategy (astrocyte Nrf2 overexpression) in concert with a clinically relevant model for *ex vivo* gene therapy. NPC can be derived from human embryonic stem cells (Carpenter *et al*., 2001; Reubinoff *et al*., 2001; Zhang *et al*., 2001), isolated from human fetuses (Uchida *et al*., 2000), or potentially produced from induced pluripotent stem cells. These sources for NPC make it possible to obtain the necessary number and quality of cell cultures for clinical application. Arguments for the use of NPC in *ex vivo* gene therapy have been made previously (Capowski *et al*., 2007; Ebert and Svendsen, 2005). In previous work, our laboratory found that human NPCs exhibit an intact system for Nrf2 responsiveness, which subsequently results in resistance to H_2O_2 (Li *et al*., 2005). Additionally, our group used Nrf2-overexpressing primary astrocytes grafted into striatum to show protection from malonate and 6-OHDA toxicity (Calkins *et al*., 2005; Jakel *et al*., 2005). Based on this work, mouse NPCs were isolated and EGF-propagated neurospheres were established (Martens, *et al*., 2000, Tropepe, *et al*., 1999). We hypothesized that stable grafts of Nrf2-overexpressing NPC in striatum would protect from malonate toxicity. Indeed, this was the case. Striata receiving Ad-Nrf2–transduced NPC grafts were protected from malonate when compared to striata grafted with Ad-GFP–transduced NPC. To the best of our knowledge, all cells that comprised the stable grafts were astrocytes. GFP labeling was used to assess survival and cell type of the NPC postgrafting. All GFP-positive cells exhibited an astrocyte-like morphology, and all GFP-positive cells colabeled with the astrocyte-specific marker GFAP. Therefore, we conclude that virtually all the grafted cells retaining the *ex vivo* modification were subject to an astrocytic fate.

Astrocytic Nrf2-dependent changes were shown to be protective when induced either before or during toxic insult. Thus, we conclude that astrocyte-specific Nrf2-mediated protection may be beneficial when initiated either before or after onset of neurodegeneration. It is well known that astrocytes play a major role in combating oxidative stress in brain. For example, it is hypothesized that glutathione levels in neurons are directly controlled by glutathione levels in astrocytes (Dringen, 2000). Furthermore, astrocytes may aid in the prevention of excitotoxicity as well as microglial activation by sequestering excess extracellular glutamate (Tilleux and Hermans, 2007). While both excitotoxicity and microglial activation are usually considered distinct from oxidative stress, it is clear that both conditions involve and are dependent on oxidative stress when leading to cell death. By enhancing the ability of astrocytes to combat oxidative stress using Nrf2 *in vivo*, we find that neurons are protected from toxic insult. The experiments described in this article further the hypothesis that astrocytic Nrf2 can protect neurons from toxicity. The mechanism of this protection has been studied *in vitro* (Kraft *et al*., 2004; Shih *et al*., 2003; Vargas *et al*., 2006); however, we now possess tools with which we may probe mechanism *in vivo* using pharmacological or genetic approaches. One key hypothesis that may be evaluated is that Nrf2-mediated protection is dependent on GSH secretion from the astrocyte. It may be possible to address this using a cross of the GFAP-Nrf2 mice with the recently characterized GCLM knockout mice (Chen *et al*., 2005; Yang *et al*., 2002). GCLM knockout mice develop normally; however, they exhibit as little as 15% of normal GSH content in brain. Furthermore, induction of the ARE in by tert-butylhydroquinone in murine embryonic fibroblast cultures from GCLM−/− animals does not lead to increased GSH production but does protect from arsenite-induced apoptosis (Kann *et al*., 2005). We would therefore expect that GFAP-Nrf2 transgenic mice on a GCLM−/−

background would exhibit increased astrocytic-Nrf2 responsiveness without increased GSH synthesis. This situation would allow us to test the ability of Nrf2 to protect from neurotoxicity in the absence of increased GSH and give mechanistic insight into Nrf2 neuroprotective capabilities.

Signaling by the Nrf2-ARE pathway may be initiated by several mechanisms not involving Nrf2 overexpression. Because of this fact, there may be multiple approaches for targeting Nrf2 as a therapeutic (Calkins *et al*., 2009). Both exogenous and endogenous molecules have demonstrated ability to activate Nrf2 signaling and induce cytoprotective genes. Two disparate examples of endogenous activators are fibroblast growth factor-1 (FGF-1) and 4-hydroxynonenol (4-HNE). FGF-1 was shown to activate Nrf2 in spinal cord astrocytes and protect motor neurons from cell death (Pehar *et al*., 2005; Vargas *et al*., 2005, 2006). 4-HNE on the other hand is a highly reactive by-product of lipid peroxidation. Accumulation of this toxic molecule activates Nrf2 and subsequently increases expression of the genes responsible for its detoxification (Ishii *et al*., 2004; Levonen *et al*., 2004). Additionally, Nrf2 is activated by a variety of bioactive food components. Molecules such as epigallocatechin 3-gallate from green tea, sulforaphane from broccoli sprouts, and curcumin from turmeric are all known to activate Nrf2 (Balogun *et al*., 2003; Kensler *et al*., 2000; Kweon *et al*., 2006; Rushmore and Kong, 2002). Because of the link between oxidative stress and cancer-causing mutations, it has been suggested that these molecules may be useful as chemopreventative agents (Chen and Kong, 2004; Kensler and Wakabayashi, 2010). Likewise, it is possible that sustained Nrf2 activation by these food components may prove to be an effective means for prevention or treatment of neurodegenerative conditions.

The observations in this article provide a strong argument for activation of astrocytic Nrf2 as a target for prevention of neurodegeneration. We show herein that neuroprotection may result from enhanced activation of Nrf2 that occurs either prior to toxic insult (as in NPC grafting) or during the pathogenic process (as in GFAP-Nrf2 transgenic mice). As such, Nrf2 targeting may be useful in protection of surviving neurons throughout the neurodegenerative process.

FUNDING

National Institute of Environmental Health Sciences (ES08089 and ES10042); Hereditary Disease Foundation (to J.A.J.); Molecular and Environmental Toxicology (pre-doctoral training grant T32 ES007015 to M.J.C.).

ACKNOWLEDGMENTS

The authors would like to thank Jon M. Resch, Hoa Ahn Phan, and Sara Amirahmadi for maintaining mouse colonies.

REFERENCES

Balogun, E., Hoque, M., Gong, P., Killeen, E., Green, C. J., Foresti, R., Alam, J., and Motterlini, R. (2003). Curcumin activates the haem oxygenase-1 gene via regulation of Nrf2 and the antioxidant-responsive element. *Biochem. J*. **371,** 887–895.

Beal, M. F., Brouillet, E., Jenkins, B., Henshaw, R., Rosen, B., and Hyman, B. T. (1993a). Age-dependent striatal excitotoxic lesions produced by the endogenous mitochondrial inhibitor malonate. *J. Neurochem.* **61,** 1147–1150.

Beal, M. F., Brouillet, E., Jenkins, B. G., Ferrante, R. J., Kowall, N. W., Miller, J. M., Storey, E., Srivastava, R., Rosen, B. R., and Hyman, B. T. (1993). Neurochemical and histologic characterization of striatal excitotoxic lesions produced by the mitochondrial toxin 3-nitropropionic acid. *J. Neurosci.* **13,** 4181–4192.

Brenner, M., and Messing, A. (1996). GFAP transgenic mice. *Methods* **10,** 351–364.

Brouillet, E., Jenkins, B. G., Hyman, B. T., Ferrante, R. J., Kowall, N. W., Srivastava, R., Roy, D. S., Rosen, B. R., and Beal, M. F. (1993). Age-dependent vulnerability of the striatum to the mitochondrial toxin 3-nitropropionic acid. *J. Neurochem.* **60,** 356–359.

Burton, N. C., Kensler, T. W., and Guilarte, T. R. (2006). In vivo modulation of the Parkinsonian phenotype by Nrf2. *Neurotoxicology* **27,** 1094–1100.

Calkins, M. J., Jakel, R. J., Johnson, D. A., Chan, K., Kan, Y. W., and Johnson, J. A. (2005). Protection from mitochondrial complex II inhibition in vitro and in vivo by Nrf2-mediated transcription. *Proc. Natl. Acad. Sci. U.S.A.* **102,** 244–249.

Calkins, M. J., Johnson, D. A., Townsend, J. A., Vargas, M. R., Dowell, J. A., Williamson, T. P., Kraft, A. D., Lee, J. M., Li, J., and Johnson, J. A. (2009). The Nrf2/ARE pathway as a potential therapeutic target in neurodegenerative disease. *Antioxid. Redox Signal* **11,** 497–508.

Capowski, E. E., Schneider, B. L., Ebert, A. D., Seehus, C. R., Szulc, J., Zufferey, R., Aebischer, P., and Svendsen, C. N. (2007). Lentiviral vector-mediated genetic modification of human neural progenitor cells for ex vivo gene therapy. *J. Neurosci. Methods* **163,** 338–349.

Carpenter, M. K., Inokuma, M. S., Denham, J., Mujtaba, T., Chiu, C. P., and Rao, M. S. (2001). Enrichment of neurons and neural precursors from human embryonic stem cells. *Exp. Neurol.* **172,** 383–397.

Chen, C., and Kong, A. N. (2004). Dietary chemopreventive compounds and ARE/EpRE signaling. *Free Radic. Biol. Med.* **36,** 1505–1516.

Chen, P. C., Vargas, M. R., Pani, A. K., Smeyne, R. J., Johnson, D. A., Kan, Y. W., and Johnson, J. A. (2009). Nrf2-mediated neuroprotection in the MPTP mouse model of Parkinson's disease: critical role for the astrocyte. *Proc. Natl. Acad. Sci. U.S.A.* **106,** 2933–2938.

Chen, Y., Shertzer, H. G., Schneider, S. N., Nebert, D. W., and Dalton, T. P. (2005). Glutamate cysteine ligase catalysis: dependence on ATP and modifier subunit for regulation of tissue glutathione levels. *J. Biol. Chem.* **280,** 33766–33774.

Dringen, R. (2000). Metabolism and functions of glutathione in brain. *Prog. Neurobiol.* **62,** 649–671.

Ebert, A. D., and Svendsen, C. N. (2005). A new tool in the battle against Alzheimer's disease and aging: ex vivo gene therapy. *Rejuvenation Res.* **8,** 131–134.

Ishii, T., Itoh, K., Ruiz, E., Leake, D. S., Unoki, H., Yamamoto, M., and Mann, G. E. (2004). Role of Nrf2 in the regulation of CD36 and stress protein expression in murine macrophages: activation by oxidatively modified LDL and 4-hydroxynonenal. *Circ. Res.* **94,** 609–616.

Itoh, K., Chiba, T., Takahashi, S., Ishii, T., Igarashi, K., Katoh, Y., Oyake, T., Hayashi, N., Satoh, K., Hatayama, I., *et al.* (1997). An Nrf2/small Maf heterodimer mediates the induction of phase II detoxifying enzyme genes

through antioxidant response elements. *Biochem. Biophys. Res. Commun.* **236,** 313–322.

Itoh, K., Wakabayashi, N., Katoh, Y., Ishii, T., Igarashi, K., Engel, J. D., and Yamamoto, M. (1999). Keap1 represses nuclear activation of antioxidant responsive elements by Nrf2 through binding to the amino-terminal Neh2 domain. *Genes Dev.* **13,** 76–86.

Jakel, R. J., Kern, J. T., Johnson, D. A., and Johnson, J. A. (2005). Induction of the protective antioxidant response element pathway by 6-hydroxydopamine in vivo and in vitro. *Toxicol. Sci.* **87,** 176–186.

Jakel, R. J., Townsend, J. A., Kraft, A. D., and Johnson, J. A. (2007). Nrf2-mediated protection against 6-hydroxydopamine. *Brain Res.* **1144,** 192–201.

Johnson, D. A., Andrews, G. K., Xu, W., and Johnson, J. A. (2002). Activation of the antioxidant response element in primary cortical neuronal cultures derived from transgenic reporter mice. *J. Neurochem.* **81,** 1233–1241.

Kann, S., Estes, C., Reichard, J. F., Huang, M. Y., Sartor, M. A., Schwemberger, S., Chen, Y., Dalton, T. P., Shertzer, H. G., Xia, Y., *et al.* (2005). Butylhydroquinone protects cells genetically deficient in glutathione biosynthesis from arsenite-induced apoptosis without significantly changing their prooxidant status. *Toxicol. Sci.* **87,** 365–384.

Kensler, T. W., Curphey, T. J., Maxiutenko, Y., and Roebuck, B. D. (2000). Chemoprotection by organosulfur inducers of phase 2 enzymes: dithiolethiones and dithiins. *Drug Metabol. Drug Interact.* **17,** 3–22.

Kensler, T. W., and Wakabayashi, N. (2010). Nrf2: friend or foe for chemoprevention? *Carcinogenesis* **31,** 90–99.

Kensler, T. W., Wakabayashi, N., and Biswal, S. (2007). Cell survival responses to environmental stresses via the Keap1-Nrf2-ARE pathway. *Annu. Rev. Pharmacol. Toxicol.* **47,** 89–116.

Kobayashi, A., Kang, M. I., Okawa, H., Ohtsuji, M., Zenke, Y., Chiba, T., Igarashi, K., and Yamamoto, M. (2004). Oxidative stress sensor Keap1 functions as an adaptor for Cul3-based E3 ligase to regulate proteasomal degradation of Nrf2. *Mol. Cell. Biol.* **24,** 7130–7139.

Kraft, A. D., Johnson, D. A., and Johnson, J. A. (2004). Nuclear factor E2-related factor 2-dependent antioxidant response element activation by tert-butylhydroquinone and sulforaphane occurring preferentially in astrocytes conditions neurons against oxidative insult. *J. Neurosci.* **24,** 1101–1112.

Kraft, A. D., Lee, J. M., Johnson, D. A., Kan, Y. W., and Johnson, J. A. (2006). Neuronal sensitivity to kainic acid is dependent on the Nrf2-mediated actions of the antioxidant response element. *J. Neurochem.* **98,** 1852–1865.

Kweon, M. H., Adhami, V. M., Lee, J. S., and Mukhtar, H. (2006). Constitutive overexpression of Nrf2-dependent heme oxygenase-1 in A549 cells contributes to resistance to apoptosis induced by epigallocatechin 3-gallate. *J. Biol. Chem.* **281,** 33761–33772.

Lee, J. M., Shih, A. Y., Murphy, T. H., and Johnson, J. A. (2003). NF-E2-related factor-2 mediates neuroprotection against mitochondrial complex I inhibitors and increased concentrations of intracellular calcium in primary cortical neurons. *J. Biol. Chem.* **278,** 37948–37956.

Levonen, A. L., Landar, A., Ramachandran, A., Ceaser, E. K., Dickinson, D. A., Zanoni, G., Morrow, J. D., and Darley-Usmar, V. M. (2004). Cellular mechanisms of redox cell signalling: role of cysteine modification in controlling antioxidant defences in response to electrophilic lipid oxidation products. *Biochem. J.* **378,** 373–382.

Li, J., Johnson, D., Calkins, M., Wright, L., Svendsen, C., and Johnson, J. (2005). Stabilization of Nrf2 by tBHQ confers protection against oxidative stress-induced cell death in human neural stem cells. *Toxicol. Sci.* **83,** 313–328.

Martens, D. J., Tropepe, V., and van Der Kooy, D. (2000). Separate proliferation kinetics of fibroblast growth factor-responsive and epidermal growth factor-responsive neural stem cells within the embryonic forebrain germinal zone. *J. Neurosci.* **20,** 1085–1095.

Pehar, M., Vargas, M. R., Cassina, P., Barbeito, A. G., Beckman, J. S., and Barbeito, L. (2005). Complexity of astrocyte-motor neuron interactions in amyotrophic lateral sclerosis. *Neurodegener. Dis.* **2,** 139–146.

Reubinoff, B. E., Itsykson, P., Turetsky, T., Pera, M. F., Reinhartz, E., Itzik, A., and Ben-Hur, T. (2001). Neural progenitors from human embryonic stem cells. *Nat. Biotechnol.* **19,** 1134–1140.

Rietze, R. L., and Reynolds, B. A. (2006). Neural stem cell isolation and characterization. *Methods Enzymol.* **419,** 3–23.

Rushmore, T. H., and Kong, A. N. (2002). Pharmacogenomics, regulation and signaling pathways of phase I and II drug metabolizing enzymes. *Curr. Drug Metab.* **3,** 481–490.

Rushmore, T. H., Morton, M. R., and Pickett, C. B. (1991). The antioxidant responsive element. Activation by oxidative stress and identification of the DNA consensus sequence required for functional activity. *J. Biol. Chem.* **266,** 11632–11639.

Rushmore, T. H., and Pickett, C. B. (1990). Transcriptional regulation of the rat glutathione S-transferase Ya subunit gene. Characterization of a xenobiotic-responsive element controlling inducible expression by phenolic antioxidants. *J. Biol. Chem.* **265,** 14648–14653.

Satoh, T., Kosaka, K., Itoh, K., Kobayashi, A., Yamamoto, M., Shimojo, Y., Kitajima, C., Cui, J., Kamins, J., Okamoto, S., *et al.* (2008). Carnosic acid, a catechol-type electrophilic compound, protects neurons both in vitro and in vivo through activation of the Keap1/Nrf2 pathway via S-alkylation of targeted cysteines on Keap1. *J. Neurochem.* **104,** 1116–1131.

Satoh, T., Okamoto, S. I., Cui, J., Watanabe, Y., Furuta, K., Suzuki, M., Tohyama, K., and Lipton, S. A. (2006). Activation of the Keap1/Nrf2 pathway for neuroprotection by electrophilic [correction of electrophillic] phase II inducers. *Proc. Natl. Acad. Sci. U.S.A.* **103,** 768–773.

Shih, A. Y., Imbeault, S., Barakauskas, V., Erb, H., Jiang, L., Li, P., and Murphy, T. H. (2005a). Induction of the Nrf2-driven antioxidant response confers neuroprotection during mitochondrial stress in vivo. *J. Biol. Chem.* **280,** 22925–22936.

Shih, A. Y., Johnson, D. A., Wong, G., Kraft, A. D., Jiang, L., Erb, H., Johnson, J. A., and Murphy, T. H. (2003). Coordinate regulation of glutathione biosynthesis and release by Nrf2-expressing glia potently protects neurons from oxidative stress. *J. Neurosci.* **23,** 3394–3406.

Shih, A. Y., Li, P., and Murphy, T. H. (2005b). A small-molecule-inducible Nrf2-mediated antioxidant response provides effective prophylaxis against cerebral ischemia in vivo. *J. Neurosci.* **25,** 10321–10335.

Tietze, F. (1969). Enzymic method for quantitative determination of nanogram amounts of total and oxidized glutathione: applications to mammalian blood and other tissues. *Anal. Biochem.* **27,** 502–522.

Tilleux, S., and Hermans, E. (2007). Neuroinflammation and regulation of glial glutamate uptake in neurological disorders. *J. Neurosci. Res.* **85,** 2059–2070.

Tropepe, V., Sibilia, M., Ciruna, B. G., Rossant, J., Wagner, E. F., and van der Kooy, D. (1999). Distinct neural stem cells proliferate in response to EGF and FGF in the developing mouse telencephalon. *Dev. Biol.* **208,** 166–188.

Uchida, N., Buck, D. W., He, D., Reitsma, M. J., Masek, M., Phan, T. V., Tsukamoto, A. S., Gage, F. H., and Weissman, I. L. (2000). Direct isolation of human central nervous system stem cells. *Proc. Natl. Acad. Sci. U.S.A.* **97,** 14720–14725.

Vargas, M. R., Johnson, D. A., Sirkis, D. W., Messing, A., and Johnson, J. A. (2008). Nrf2 activation in astrocytes protects against neurodegeneration in mouse models of familial amyotrophic lateral sclerosis. *J. Neurosci.* **28,** 13574–13581.

Vargas, M. R., Pehar, M., Cassina, P., Beckman, J. S., and Barbeito, L. (2006). Increased glutathione biosynthesis by Nrf2 activation in astrocytes prevents p75NTR-dependent motor neuron apoptosis. *J. Neurochem.* **97,** 687–696.

Vargas, M. R., Pehar, M., Cassina, P., Martinez-Palma, L., Thompson, J. A., Beckman, J. S., and Barbeito, L. (2005). Fibroblast growth factor-1 induces

heme oxygenase-1 via nuclear factor erythroid 2-related factor 2 (Nrf2) in spinal cord astrocytes: consequences for motor neuron survival. *J. Biol. Chem.* **280,** 25571–25579.

Wu, D. C., Teismann, P., Tieu, K., Vila, M., Jackson-Lewis, V., Ischiropoulos, H., and Przedborski, S. (2003). NADPH oxidase mediates oxidative stress in the 1-methyl-4-phenyl-1,2,3,6-tetrahydropyridine model of Parkinson's disease. *Proc. Natl. Acad. Sci. U.S.A.* **100,** 6145–6150.

Yang, Y., Dieter, M. Z., Chen, Y., Shertzer, H. G., Nebert, D. W., and Dalton, T. P. (2002). Initial characterization of the glutamate-cysteine ligase modifier subunit Gclm(−/−) knockout mouse. Novel model system for a severely compromised oxidative stress response. *J. Biol. Chem.* **277,** 49446–49452.

Zhang, S. C., Wernig, M., Duncan, I. D., Brustle, O., and Thomson, J. A. (2001). In vitro differentiation of transplantable neural precursors from human embryonic stem cells. *Nat. Biotechnol.* **19,** 1129–1133.